Anticancer activity and green synthesized SeO_2 Nanoparticles from Cinnamomum verum bark extract

Inbaththamizhan M[1], John Kishore D[2], Krashan K[3], Sugitha B[4], Vijayakumar D[5]
UG Students, Department of Biomedical Engineering, Mahendra Institute of Technology, Namakkal – 637503 Tamilnadu.
Associate Professor, Department of Biomedical, Mahendra Institute of Technology, Namakkal – 637503 Tamilnadu.

Abstract- *Selenium is an important component of human diet and numerous studies have declared its chemopreventive and therapeutic properties against cancer. However, very limited studies have been conducted about the properties of selenium nanostructured materials. Here, we have shown that the anticancer property of green synthesized selenium nanoparticles from Cinnamon. The optical, structural, morphological, elemental, and functional characterizations of the SeO2NPs were carried out using techniques such as UV-vis spectrophotometry, electron microscopy, energy dispersive X-ray spectrometry, and Fourier transform infrared spectrophotometry, respectively. The results showed the presence of spherical shape of SeO2 nanoparticles with 149 nm of nanoparticle particle size. The MTT (3-(4,5-dimethylthiazol-2-yl)-2,5-diphenyltetrazolium bromide) assay revealed that the biosynthesized SeO2NP induces cell death of Hep-G2 human cancer cells. The IC50 value was recorded at 55.16 µg/mL, respectively. Furthermore, the EtBr/Ao staining results confirmed that the selenium nanoparticles induced apoptosis of cancer cells. Therefore, the SeO2 NPs could be a promising candidate for the control of cancer cells.*

Keywords- biosynthesis, selenium NPs, anticancer activity, Cinnamon

I. INTRODUCTION

Cancer is a disease in which abnormal cells divide uncontrollably and destroy body tissue. Cancer is a disease that occurs when cells grow and divide abnormally, causing a growth called a tumor. Cancer is caused by mutations to the DNA within cells, which can cause the cell to stop its normal function. There are more than 200 different types of cancer, which are divided into groups according to the type of cell they start from. The five main cancer groups are: Carcinomas, Lymphomas, Leukaemias, Brain tumors, and Sarcomas.

Hepatocellular Carcinoma (HCC)

Cancer that begins in the cells of the liver. The liver is the football-sized organ in the upper-right area of the stomach. Liver cancer, also known as hepatic cancer, is a malignant tumor that starts in the liver. It can be primary, meaning it starts in the liver, or secondary, meaning it spreads from another part of the body to the liver. The most common type of primary liver cancer is hepatocellular carcinoma (HCC), which affects the liver's main cell type, hepatocytes. Most common primary malignant tumor of the liver. Asia and Japan > United States. Etiology: Cirrhosis, Hepatitis B and C virus, Alcohol, AlfatoxinB1. Tendency for Hematogenous spread and invasion of portal and hepatic veins. Tumor marker: Alpha - Fetoprotein. HCC and CCC comprise the overwhelming majority of primary malignant hepatic neoplasms. Secondary or metastatic hepatic neoplasms are especially common owing to the blood filtration function of the liver. Both HCC and CCC are slow-growing tumors but majority of patients are unresectable at presentation.

Cinnamon has antioxidant, anti-inflammatory, antidiabetic, antimicrobial, anticancer, lipid-lowering, and cardiovascular-disease-lowering compound. Cinnamaldehyde exhibited potent antiproliferative effect on a liver cancer cell line, HepG2, in a dose- and time-dependent pattern where a concentration of 30 µM of cinnamaldehyde inhibited approximately 71% of cell proliferation.

A nanoparticle is a particle of matter with a diameter of 1–100 nanometers (nm). Nanoparticles are spherical, polymeric particles composed of natural or artificial polymers. They range in size between 10 and 500 nm. As a consequence of their spherical shape and high surface area to volume ratio, these particles have a wide range of potential applications. Selenium nanoparticles (SeNPs) are a potential nutritional supplement due to their low toxicity and ability to gradually release selenium after ingestion. selenium can significantly suppress liver cancer carcinogenesis induced by aflatoxin B1, dimethyl azobenzene, or acetylamino.

Green synthesis is a sustainable and environmentally friendly method for producing nanoparticles. Green chemistry, similar to sustainable chemistry or circular chemistry, is an area of chemistry and chemical engineering focused on the design of products and processes that minimize or eliminate the use and generation of hazardous substances.

II. AIM

To find the anticancer property of SeO2 obtain using Cinnamomum verum against hepG2 cells

III. OBJECTIVES

1) Collection and Authentication of bark material
2) Extraction of Bark Material
3) Green synthesis of SeO2 nanoparticles using process and plant different ratios
4) Bulk synthesis of SeO2 nanoparticles
5) Characterization of and SeO2 nanoparticles by
   - ❖ SEM – (Scanning Electron Microscopy)
   - ❖ XRD – (X-ray diffraction analysis)
   - ❖ FTIR – (Fourier Transform Infrared spectroscopy)
   - ❖ DLS – (Dynamic Light Scattering)
   - ❖ UV – (Ultraviolet)
6) Anticancer activity of nanoparticles by MTT assay in Hep G2 cell line.
7) EtBr/Ao staining of fluorescent imaging method.

IV. METHODOLOGY

1) Collection and Identification of Plants

Cinnamon bark was collected from Mallasamudram, Namakkal district, TamilNadu, India in the month of August, 2023. The plant material was identified and authenticated by Department of Biomedical Dr. D.Vijayakumar Assistant Professor, Mahendra Institue of Technology Namakkal, TamilNadu, India.

Collection of Cinnamomum verum

2) Preparation of aqueous extract of Cinnamon:

1gm of Barks of Cinnamon were used for green synthesis of Cinnamon was homogenized into fine powder and boiled with 100 ml Double distilled water for 20 min at 100°C and the extract was obtained after filtration through Muslin cloth and No. 1 filter paper and was used for green synthesis experiments.

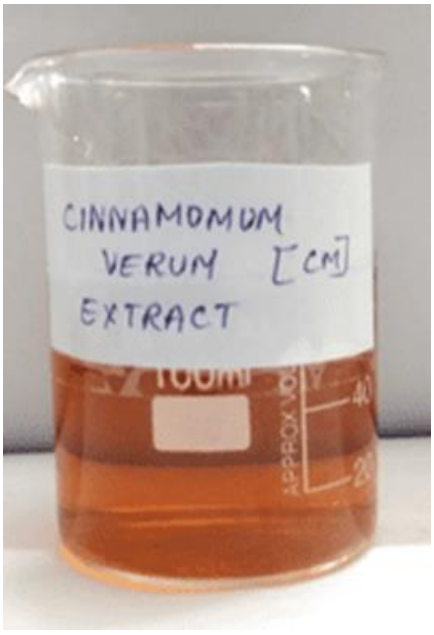

Figure.1 Plant extract (CM)

3) Preparation of 1mM Sodium Selenite Solution:

For the preparation of ImM Sodium Selenite (Na2SeO3), 0.0421gms of Na2SeO3 was dissolved in 100 ml of double distilled water. The solution was mixed completely and stored in yellow colored bottle to prevent auto oxidation of sodium.

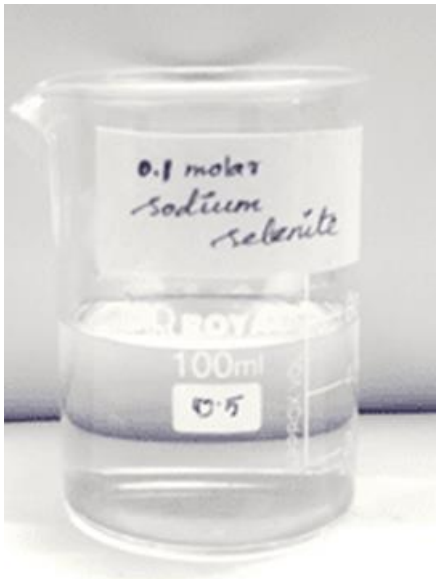

Figure.2 0.1 M of Sodium selenite

Synthesis of Sodium Selenite Nanoparticles using Cinnamomum verum Barks Extract:

15ml of Cinnamomum verum plants barks extract was added to 35 ml of 1mM aqueous sodium selenite (Na2Seo3) solution and bolied at 100 c temperature at 10mins for 24hrs in Dark Conditions to produce sodium selenite nanoparticles.

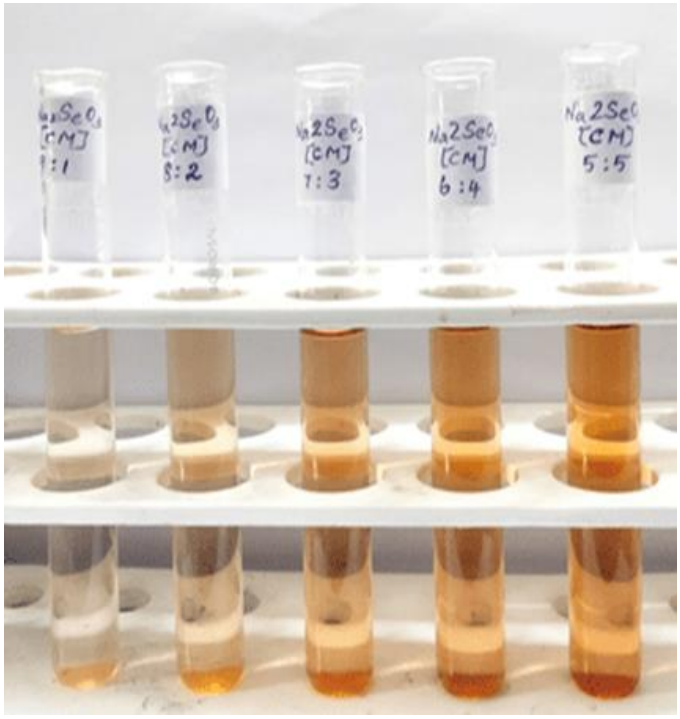

Figure.3 Synthesis of SeO2 NPs using Sodium selenite + (CM) Plant extract in a differentratios

Figure.4 Alkaline treatment -NaOH (100µL)

Figure.5 Optimization of SeO2 NPs at various Ph

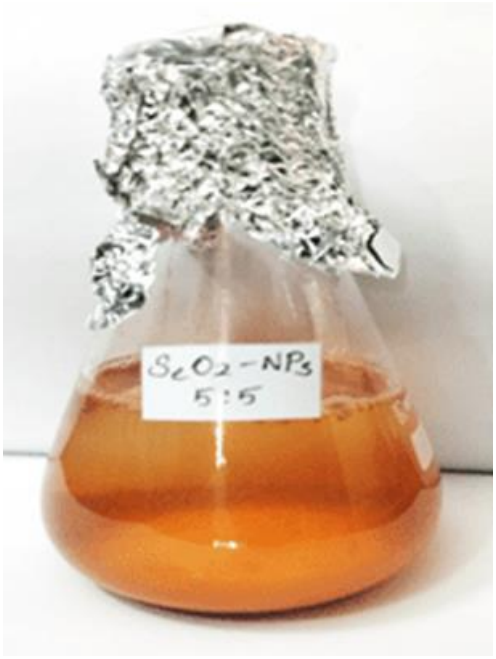

Figure.6 Bulk production using Sodium selenite + (CM) plant extract

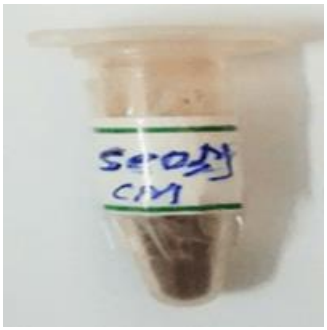

Figure.7 Synthesized SeO2 NPs

4) Characterization of synthesized Na2SeO3 nanoparticles:

The biosynthesized Sodium Selenite were characterized according to the method described by Gurunathan et al. UV-vis spectra were measured using A The shape and size of sodium selenite nanoparticles were determined by TEM. For TEM, a drop of aqueous sodium selenite nanoparticles sample was fixed on a carbon coated grid, and let dry in room temperature; the micrographs were acquired using TEM. Fourier Transform infrared spectroscopy (FT- IR) (Thermo Scientific Smart ITR ™) was utilized to describe the changes and the number on the face of the synthesized nanoparticles.

5) MTT ASSAY

Principle

MTT (3-4, 5 dimethylthiazol-2yl-2, 5-diphenyl tetrazolium bromide) assay, is based on the ability of a mitochondrial dehydrogenase enzyme of viable cells to cleave the tetrazolium rings of the pale yellow MTT and form a dark blue colored formazan crystal which is largely impermeable to cell membranes, thus resulting in its accumulation within healthy cells [7]. Solubilization of cells by the addition of detergents (DMSO) results in the liberation of crystals which are solubilized. The number of surviving cells is directly proportional to the level of formazan product created [8]. The color can be quantified using a multi-well plate reader. Materials required: Fetal Bovine Serum (FBS) and antibiotic solution were from Gibco (USA), DMSO (Dimethyl sulfoxide) and MTT (3-4,5 dimethylthiazol-2yl-2,5-diphenyl tetrazolium bromide) (5 mg/ml) were from Sigma, (USA), DMEM medium, 1X PBS, (India) [9]. 96 well tissue culture plate and wash beaker were from Tarson (India) [10].

PROCEDURE

Cell culture

Hep-G2 liver cancer cell line was purchased from NCCS, Pune and were cultured in liquid medium (DMEM) supplemented 10% Fetal Bovine Serum (FBS), 100 µg/ml penicillin and 100 µg/ml streptomycin, and maintained under an atmosphere of 5% CO2 at 37oC.

MTT assay

The Test sample was tested for in vitro cytotoxicity, using Hep-G2 liver cells by MTT assay. Briefly, the cultured Hep-G2 liver cells were harvested by trypsinization and pooled in a 15 ml tube [11]. Then, the cells were plated at a density of 1×105 cells/ml cells/well (200 µL) into the 96-well tissue culture plate in DMEM medium containing 10 % FBS and 1% antibiotic solution for 24-48 hour at 37°C. The wells were washed with sterile PBS and treated with the Test sample in a serum free DMEM medium [12]. Each sample was replicated three times and the cells were incubated at 37°C in a humidified 5% CO2 incubator for 24 h. After incubation, MTT (10 µL of 5 mg/ml) was added to each well and the cells were incubated for another 2-4 h until purple precipitates were clearly visible under an inverted microscope [13]. Finally, the medium together with MTT (220 µL) was aspirated off the wells and washed with 1X PBS (200 µl). Furthermore, to dissolve formazan crystals, DMSO (100 µL) was added and the plate was shaken for 5 min [14]. The absorbance for each well was measured at 570 nm using a microplate reader (Thermo Fisher Scientific, USA) and the percentage cell viability and IC50 value were calculated using Graph Pad Prism 6.0 software (USA).

Formula Cell viability % = Test OD/Control OD X 100

6) ETBR/AO STAINING

Principle:

Fluorescent dyes with aromatic amino or guanidine groups, such as acridine orange (AO), interact with nucleotides to emit fluorescence. EtBr molecules intercalate inside the DNA double helix [15]. AO can form complexes with either double-stranded
DNA or single-stranded DNA and RNA. One molecule of AO can also interact with one phosphate group of single-stranded DNA or RNA to form an aggregated, or stacked, structure that emits red fluorescence with the maximum wavelength at 650 nm. This fluorescent dye is impermeable through the cell membranes of viable cells and can be used as fluorescent indicators of dead cells. Acridine orange is a vital dye and will stain both live and dead cells [16]. Necrotic cells stain orange but have a nuclear morphology resembling that of viable cells, with no condensed chromatin [17]. Ethidium bromide (EtBr) is only taken up by cells when cytoplasmic membrane integrity is lost and stains the nucleus red. EtBr also dominates over AO. Thus, live cells have a normal green nucleus; early apoptotic cells have a bright green nucleus with condensed or fragmented chromatin; late apoptotic cells display condensed and fragmented orange chromatin; cells that have died from direct necrosis have a structurally normal orange nucleus [18]. Ethidium re-emits this energy as yellow/orange light centered at 590 nm. The fluorescence of ethidium bromide in an aqueous solution is significantly lower than that of the intercalated dye.

Materials required

DMEM medium, Penicillin/Streptomycin antibiotic solution, Trypsin-EDTA was purchased from Gibco (USA), EtBr, and Acridine orange was purchased from Sigma Aldrich (USA), Fluorescent Imaging System, (ZOE, Bio-Rad, USA).

Procedure

Cell culture

Hep-G2 liver cell line was purchased from NCCS, Pune and was cultured in liquid medium (DMEM) supplemented 10% Fetal Bovine Serum (FBS), 100 u/ml penicillin, and 100 µg/ml streptomycin, and maintained under an atmosphere of 5% CO2 at 37oC [19].

EtBr/AO staining

Briefly, 5 x 105 cells/ml of Hep-G2 liver cells were plated into a 96 well tissue culture plate and incubated for 24 hr in a DMEM growth medium. After incubation, the cells were treated with 44.85 µg/ml of TiO2 sample in a serum-free DMEM medium [20]. The plate was incubated at 37oC at a 5% Co2 incubator for 24 hours [24]. After incubation, 10 µl of 1 mg/ml acridine orange and ethidium bromide were added to the wells and mixed gently [21]. Finally, the plate was centrifuged at 800 rpm for 2 minutes and evaluated immediately within an hour, and examined at least 100 cells by a Fluorescent Imaging System, (ZOE, Bio-Rad, USA).

V. Results

Characterization of synthesized Seo2 Nanoparticles

1) Scanning Electron Microscopy (SEM)

In the SEM images, a microscope is used to qualitatively identify the microstructural developments in the matrix of the stabilized soil specimens [21]. The SEM images of SeO2 are shown (different magnifications); thus, the spherical shape microstructure is easily observed since the pictures can be enlarged [22].

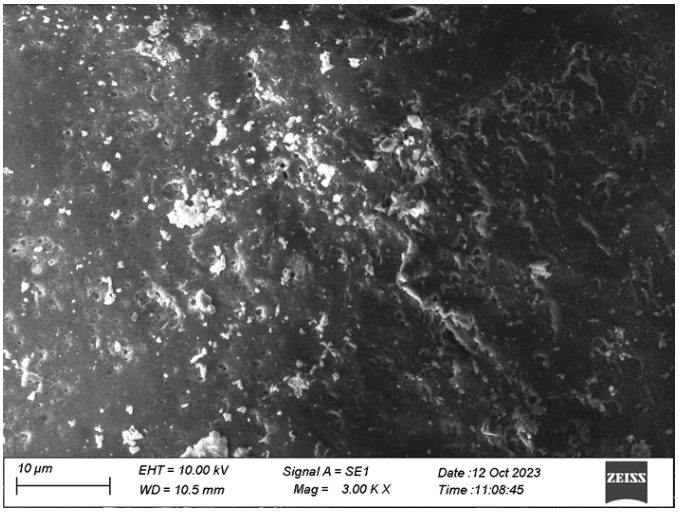

SEM (SeO2 NPs – Cinnamon) Figure.1

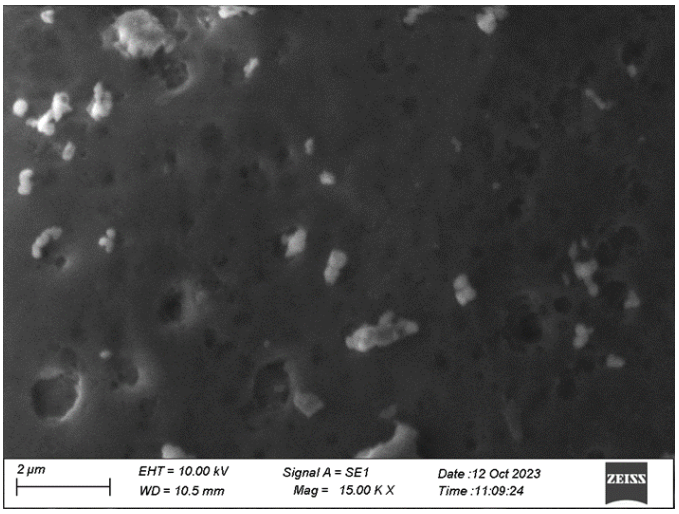

SEM (SeO2 NPs – Cinnamon) Figure.2

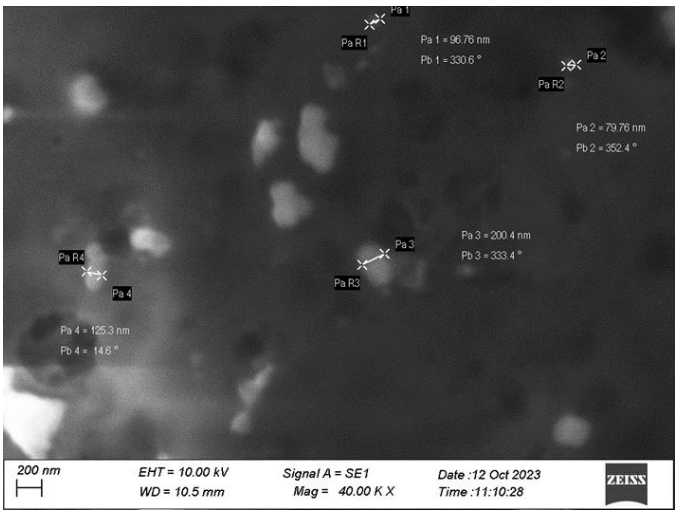

SEM (SeO2 NPs – Cinnamon) Figure.3

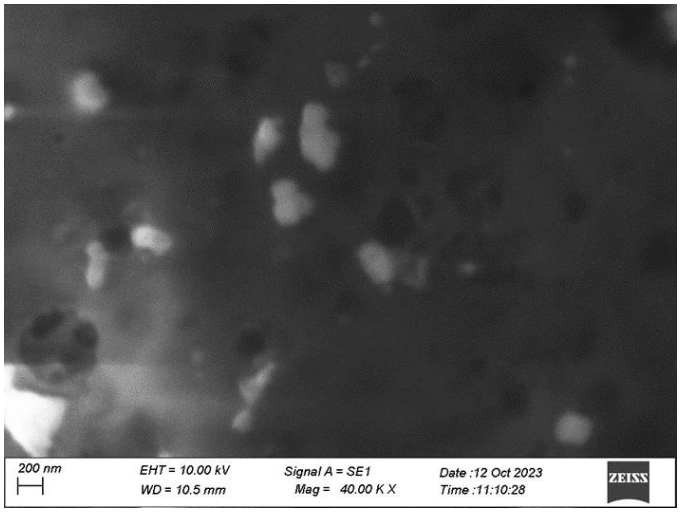

SEM (SeO2 NPs – Cinnamon) Figure.4

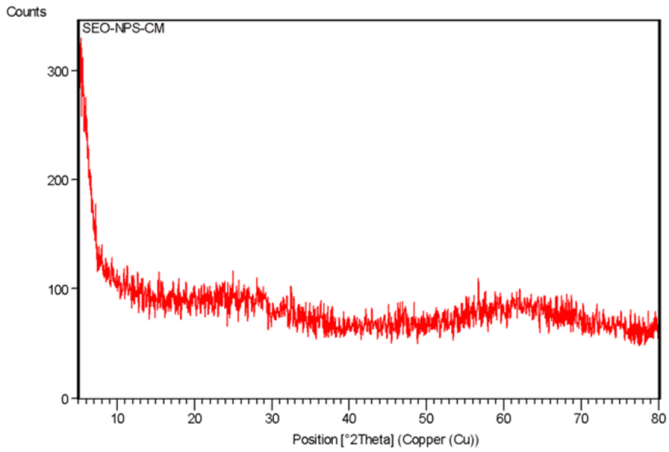

Main Graphics, Analyze View

2) X-ray diffraction (XRD)

X-ray diffraction is used most frequently to investigate the structure of bio composites with embedded nanostructure.

Dataset Name	SEO-NPS-CM
File name	F:\16.10\VINCENT\SEO-NPS-CM.raw
Comment	Scan Mode: Continuous scan mode Scan Type: Locked Coupled Goniometer Stage: Phi Goniometer Control: Diffractometer Controller only Sample Changer: Unknown Sample Changer Measurement Flag: Already measured Sync. Axis: Unknown Sync Axis Beam Optics: Unknown Beam Optics Flag Monochromator: Unknown Monochromator Analyzer: Unknown Analyzer
Measurement Date / Time	10/16/2023 1:04:35 PM
Raw Data Origin	BRUKER-binary V4 (.RAW)
Scan Axis	Gonio
Start Position [°2Th.]	5.0000
End Position [°2Th.]	80.1600
Step Size [°2Th.]	0.0400
Scan Step Time [s]	13.4400
Scan Type	Pre-set time
Offset [°2Th.]	0.0000
Divergence Slit Type	Fixed
Divergence Slit Size [°]	9999.0000
Specimen Length [mm]	10.00
Receiving Slit Size [mm]	0.1000
Measurement Temperature [°C]	25.00
Anode Material	Cu
K-Alpha1 [Å]	1.54060
K-Alpha2 [Å]	1.54443
K-Beta [Å]	1.39225
K-A2 / K-A1 Ratio	0.50000
Generator Settings	30 mA, 40 kV
Diffractometer Type	Theta/Theta
Diffractometer Number	0
Goniometer Radius [mm]	240.00
Dist. Focus-Diverg. Slit [mm]	91.00
Incident Beam Monochromator	No
Spinning	No

XRD Results Chart

3) Fourier Transform Infrared Spectroscopy (FTIR):

FTIR spectroscopy is a very powerful tool with many applications, however data interpretation is not straightforward [23]. By nature, the total spectrum generated is a series function of absorbed energy response (hence the Fourier Transform portion of the name).

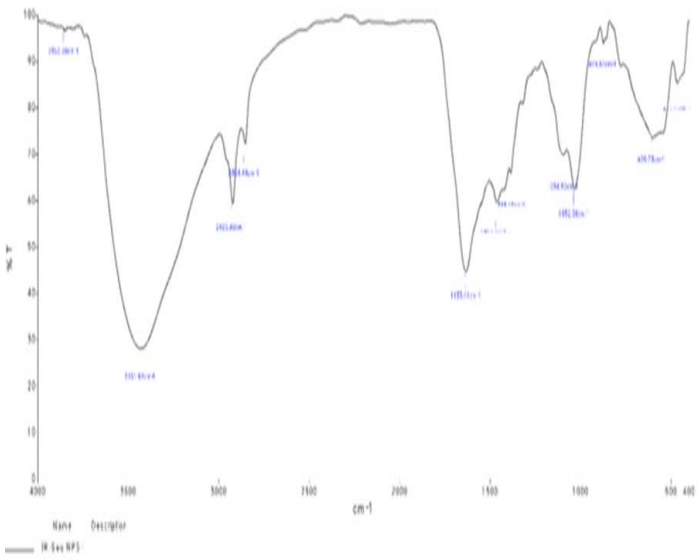

4) DLS (Dynamic Light Scattering):

Dynamic Light Scattering (DLS) analysis allows us to confidently measure the size distribution profiles of particles in the sub-micron range.

Intensity Distribution S/N : 411615

User : Common Group : Repetition : 1/1
Date : 13-Sep-23 File Name : PSA-SeO NPS
Time : 11:57:25 Sample Information :
SOP Name : SJC Size Method Security : No Security

Version 5.22 / 3.00

Intensity Distribution ACF

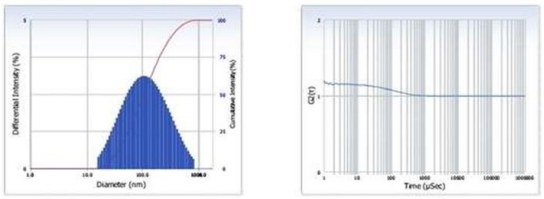

Distribution Results (Contin)

Peak	Diameter (nm)	Std. Dev.
1	163.2	149.9
2	0.0	0.0
3	0.0	0.0
4	0.0	0.0
5	0.0	0.0
Average	163.2	149.9

Residual : 2.289e-003 (O.K)

Cumulants Results
Diameter (d) : 86.1 (nm)
Polydispersity Index (P.I.) : 0.337
Diffusion Const. (D) : 5.715e-008 (cm²/sec)

Measurement Condition
Temperature : 25.0 (°C)
Diluent Name : WATER
Refractive Index : 1.3328
Viscosity : 0.8878 (cP)
Scattering Intensity : 31552 (cps)
Attenuator 1 : 10.12 (%)

Intensity Distribution Table

d (nm)	f(%)	f(cum.%)	d (nm)	f(%)	f(cum.%)	d (nm)	f(%)	f(cum.%)	d (nm)	f(%)	f(cum.%)
1.0	0.0	0.0	6.6	0.0	0.0	44.1	2.1	16.9	292.5	2.0	85.5
1.1	0.0	0.0	7.2	0.0	0.0	47.5	2.3	19.2	315.5	1.9	87.4
1.2	0.0	0.0	7.7	0.0	0.0	51.3	2.4	21.6	340.3	1.7	89.2
1.3	0.0	0.0	8.3	0.0	0.0	55.3	2.5	24.1	367.1	1.6	90.8
1.4	0.0	0.0	9.0	0.0	0.0	59.6	2.7	26.8	396.0	1.5	92.2
1.5	0.0	0.0	9.7	0.0	0.0	64.3	2.8	29.5	427.1	1.3	93.6
1.6	0.0	0.0	10.5	0.0	0.0	69.4	2.9	32.4	460.7	1.2	94.8
1.7	0.0	0.0	11.3	0.0	0.0	74.9	2.9	35.3	496.9	1.1	95.8
1.8	0.0	0.0	12.2	0.0	0.0	80.7	3.0	38.3	536.0	0.9	96.7
2.0	0.0	0.0	13.1	0.0	0.0	87.1	3.0	41.4	578.2	0.8	97.5
2.1	0.0	0.0	14.2	0.0	0.0	93.9	3.1	44.4	623.6	0.7	98.2
2.3	0.0	0.0	15.3	0.0	0.0	101.3	3.1	47.6	672.7	0.6	98.8
2.5	0.0	0.0	16.5	0.4	0.4	109.3	3.1	50.7	725.6	0.5	99.3
2.7	0.0	0.0	17.8	0.5	0.9	117.9	3.1	53.8	782.7	0.4	99.7
2.9	0.0	0.0	19.2	0.6	1.4	127.2	3.1	56.9	844.2	0.3	100.0
3.1	0.0	0.0	20.7	0.7	2.1	137.2	3.0	59.9	910.6	0.0	100.0
3.4	0.0	0.0	22.3	0.8	3.0	148.0	3.0	62.9	982.2	0.0	100.0
3.6	0.0	0.0	24.0	1.0	3.9	159.6	2.9	65.8	1059.5	0.0	100.0
3.9	0.0	0.0	25.9	1.1	5.0	172.2	2.8	68.7	1142.8	0.0	100.0
4.2	0.0	0.0	28.0	1.2	6.3	185.7	2.8	71.4	1232.7	0.0	100.0
4.5	0.0	0.0	30.2	1.4	7.6	200.3	2.7	74.1	1329.7	0.0	100.0
4.9	0.0	0.0	32.5	1.5	9.2	216.1	2.5	76.6	1434.3	0.0	100.0
5.3	0.0	0.0	35.1	1.7	10.9	233.1	2.4	79.0	1547.1	0.0	100.0
5.7	0.0	0.0	37.9	1.8	12.7	251.4	2.3	81.3	1668.7	0.0	100.0

Intensity Distribution Table

d (nm)	f(%)	f(cum.%)	d (nm)	f(%)	f(cum.%)	d (nm)	f(%)	f(cum.%)	d (nm)	f(%)	f(cum.%)
6.2	0.0	0.0	40.9	2.0	14.7	271.2	2.2	83.5	1800.0	0.0	100.0
D (10%) :	33.70	(nm)	D (50%) :	107.50	(nm)	D (90%) :	353.80	(nm)			

5) Ultra Voilet (UV):

Titanium oxide nanoparticles confirmed by observing UV-Vis peaks at 350-365nm [25].

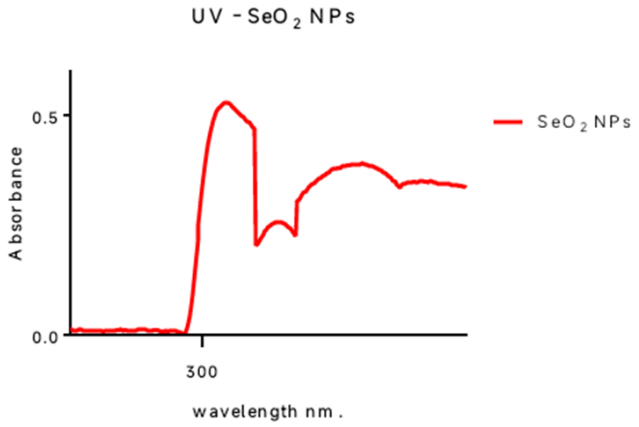

UV – VISIBLE SPECTROSCOPY ANALYSIS

	A	B	C
1	Sample Name	SeO NPs CM UV	
2	Time	September 20 16:54:58 2023	
3	Operator	TRI-BIOTECH	
4	Lamp	0	
5	Slit	0	
6	Scan From	1100.0nm	
7	Scan To	190.0nm	
8	Scan Step	1.0nm	
9	Sample Filter	10	
10	memo		
11	WL(nm)	Abs	T%
12	190	-0.0109	102.53
13	191	-0.011	102.56
14	192	-0.0105	102.45
15	193	-0.0102	102.37
16	194	-0.0123	102.87
17	195	-0.0112	102.61
18	196	-0.0103	102.4
19	197	-0.0121	102.82
20	198	-0.0118	102.75
21	199	-0.0128	102.99
22	200	-0.0125	102.93
23	201	-0.0139	103.24
24	202	-0.0115	102.68
25	203	-0.0115	102.69
26	204	-0.011	102.56
27	205	-0.011	102.57
28	206	-0.0128	102.99
29	207	-0.0143	103.35
30	208	-0.0132	103.08
31	209	-0.0107	102.5
32	210	-0.0092	102.15
33	211	-0.0097	102.25
34	212	-0.0101	102.35

6) MTT ASSAY

A. OD Value at 570 nm

S. No.	Tested sample concentration (µg/ml)	OD value at 570 nm (in triplicates)		
1	Control	2.891	2.895	2.894
2	500 µg/ml	1.591	1.619	1.629
3	400 µg/ml	1.631	1.637	1.639
4	300 µg/ml	1.797	1.741	1.774
5	200 µg/ml	1.812	1.81	1.814
6	100 µg/ml	1.921	1.928	1.93
7	80 µg/ml	1.945	1.948	1.95
8	60 µg/ml	2.005	2.024	2.028
9	40 µg/ml	2.058	2.074	2.08
10	20 µg/ml	2.108	2.117	2.129
11	10 µg/ml	2.339	2.342	2.35

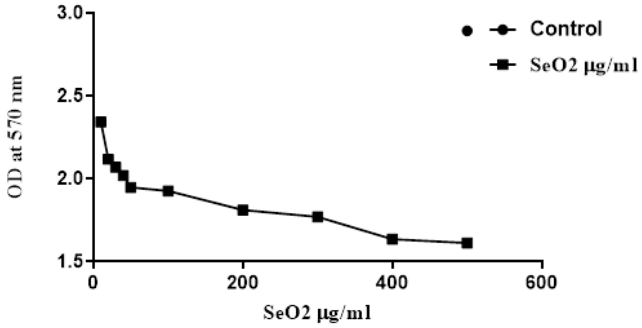

OD Value Graph

B. Cell Viability (%)

S. No.	Tested sample concentration (µg/ml)	Cell viability (%) (in triplicates)			Mean Value (%)
1	Control	100	100	100	100
2	500 µg/ml	55.0329	55.924	56.2889	55.74858
3	400 µg/ml	56.4165	56.5458	56.6344	56.532216
4	300 µg/ml	62.1584	60.1382	61.2992	61.198611
5	200 µg/ml	62.6773	62.5216	62.6814	62.626758
6	100 µg/ml	66.4476	66.5976	66.6897	66.578294
7	80 µg/ml	67.2778	67.2884	67.3808	67.315658
8	60 µg/ml	69.3532	69.9136	70.076	69.780943
9	40 µg/ml	71.1864	71.6408	71.8728	71.56668
10	20 µg/ml	72.9159	73.1261	73.566	73.202675
11	10 µg/ml	80.9063	80.8981	81.2025	81.002283

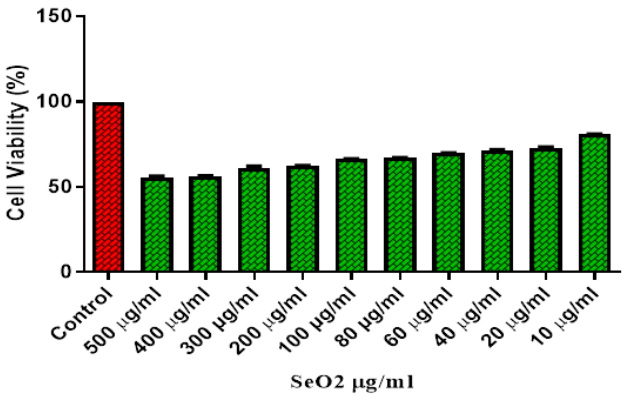

Cell Viability Graph

C. IC50 Value of tested sample is 55.16 µg/ml

log(inhibitor) vs. normalized response -- Variable slope	
Best-fit values	
LogIC50	1.742
Hill Slope	-1.062
IC50	55.16
Std. Error	
LogIC50	0.03341
Hill Slope	0.08924
95% CI (asymptotic)	
LogIC50	1.673 to 1.810
Hill Slope	-1.245 to -0.8792
IC50	47.12 to 64.57
Goodness of Fit	
Degrees of Freedom	28
R squared	0.9286
Sum of Squares	1853
Sy.x	8.135
Number of points	
# of X values	30
# Y values analysed	30

D. Images of control cells and treated cells.

Control cells	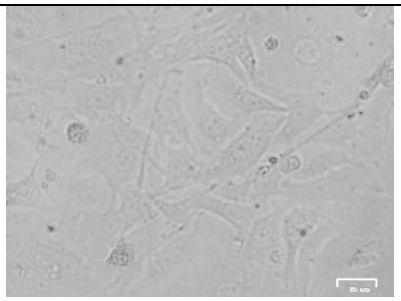

SeO2 500 µg/ml	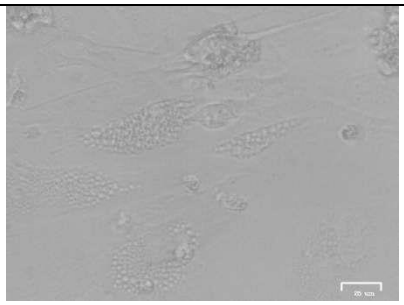
SeO2 300 µg/ml	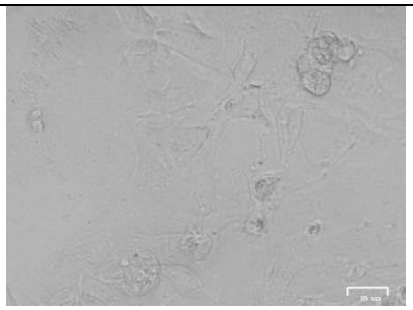
SeO2 100 µg/ml	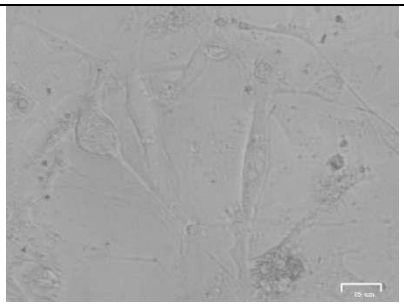
SeO2 60 µg/ml	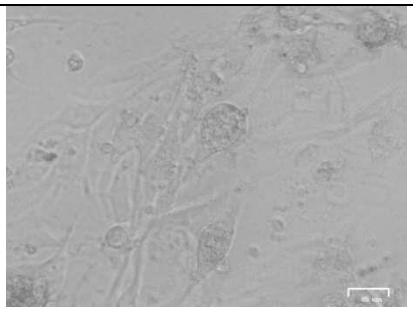
SeO2 20 µg/ml	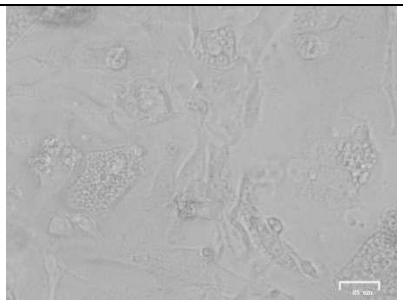

SeO2 10 µg/ml	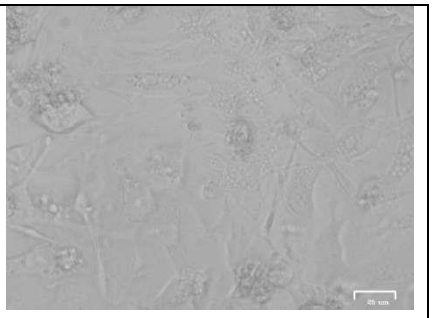

7) EtBr /AO STAINING:

Samples	Fluorescent images	Fluorescent images
Control	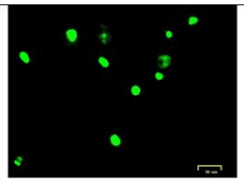	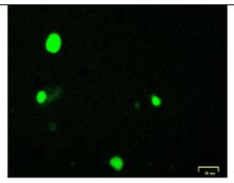
Treated with 55.16 µg/ml of SeO_2 sample	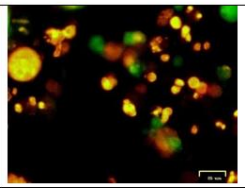	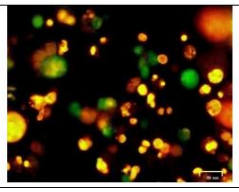

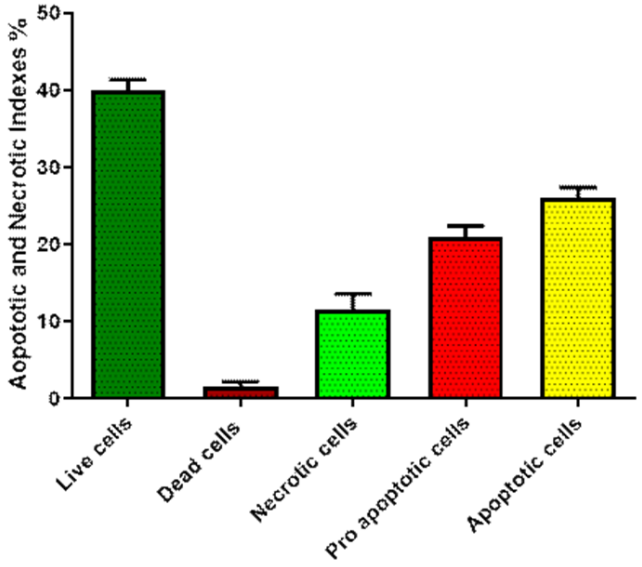

Live and Apoptotic Cells Graph

S.No	Dead cells	Necrotic cells	Pro-Apoptotic cells	Apoptotic cells	Live cells
1.	2	10	20	27	41
2.	1	13	22	25	39

VI. RESULTS AND DISCUSSION

Selenium (Se) is an important trace element that plays a crucial role in human health and regulates many crucial cellular functions mediated through its incorporation into selenoproteins. The aim of the study was to green synthesis and characterization of SeO nanoparticles from Cinnamon and their anticancer property in Hep-G2 cells. The optical, structural, morphological, elemental, and functional characterizations of the SeONPs were carried out using techniques such as UV-vis spectrophotometry, electron microscopy, energy dispersive X-ray spectrometry, and Fourier transform infrared spectrophotometry, respectively. The results showed the presence of spherical shape nanoparticles with 149 nm of particle size and the presence carboxyl groups. The MTT (3-(4,5-dimethylthiazol-2-yl)-2,5-diphenyltetrazolium bromide) assay revealed that the biosynthesized SeONP induces cell death of Hep-G2 human cancer cells. The IC50 value was recorded at 55.16 µg/mL, respectively. Furthermore, the EtBr/Ao staining results confirmed that the selenium nanoparticles induced apoptosis of cancer cells. Therefore, the SeO Nps could be a promising candidate for the control of cancer cells. Another study on the MTT (3-(4,5-dimethylthiazol-2-yl)-2,5-diphenyltetrazolium bromide) assay revealed that the biosynthesized SeNrs induces cell death of Hep-G2 and MCF-7 human cancer cells. The lethal dose (LD50%) of SeNrs on Hep-G2 and MCF-7 cells was recorded at 75.96 µg/mL and 61.86 µg/mL, respectively.

VII. CONCLUSION

In conclusion, our results clearly show a selective cytotoxicity and apoptosis inductive effect SeO Nps from cinnamon on the human hepatoma (HepG2) cell line. The isolation of the active chemical constituents from the cinnamon and determination of their individual anticancer activity will be further performed.

Acknowledgements

We acknowledge TRI-BIOTECH Trichy Research Center for characterization studies.

Conflict of Interest

The authors declare that they have ”No conflict of interest”.

REFERENCES

[1] L. L. Munn, “Cancer and infammation,” Wiley Interdiscip Rev Syst Biol Med, vol. 9, Article ID e1370, 2017.

[2] H. Nakamura and K. Takada, “Reactive oxygen species in cancer: current fndings and future directions,” Cancer Science, vol. 112, no. 10, pp. 3945–3952, 2021.

[3] M. Kubczak, A. Szustka, and M. Rogalinska, “Molecular ´ targets of natural compounds with anti-cancer properties,” International Journal of Molecular Sciences, vol. 22, no. 24, Article ID 13659, 2021.

[4] N. Singh, A. S. Rao, A. Nandal et al., “Phytochemical and pharmacological review of Cinnamomum verum J. Presla versatile spice used in food and nutrition,” Food Chemistry, vol. 338, Article ID 127773, 2021.

[5] V. B. Souza, A. T. Holkem, M. Tomazini et al., “Study of extraction kinetics and characterization of proanthocyanidin-rich extract from Ceylon cinnamon (Cinnamomum zeylanicum),” Journal of Food Processing and Preservation, vol. 45, no. 5, Article ID e15429, 2021.

[6] E. Dvorackova, M. Snoblova, L. Chromcova, and P. Hrdlicka, “Efects of extraction methods on the phenolic compounds contents and antioxidant capacities of cinnamon extracts,” Food Science and Biotechnology, vol. 24, no. 4, pp. 1201–1207, 2015.

[7] D. Bernard, A. Kwabena, O. Osei, G. Daniel, A. Sandra, and S. Elom, “Te efect of diferent drying methods on the phytochemicals and radical scavenging activity of Ceylon Cinnamon (Cinnamomum zeylanicum) plant parts,” European Journal of Medicinal Plants, vol. 4, no. 11, pp. 1324– 1335, 2014.

[8] F. Chemat, M. A. Vian, and G. Cravotto, “Green extraction of natural products: concept and principles,” International Journal of Molecular Sciences, vol. 13, no. 7, pp. 8615–8627, 2012.

[9] H. K. Kwon, J. S. Hwang, J. S. So et al., “Cinnamon extract induces tumor cell death through inhibition of NF-κB and AP1,” BMC Cancer, vol. 10, no. 1, p. 392, 2010.

[10] O. K. Yaseen and M. T. Mohammed, “Cinnamon zeylanicum aqueous improves some oxidative stress biomarkers in diabetic type 2 induced by streptozotocin in adult male albino mice,” Egyptian Journal of Chemistry, vol. 65, pp. 1-2, 2022.

[11] R. Singh, S. J. Koppikar, P. Paul, S. Gilda, A. R. Paradkar, and R. Kaul-Ghanekar, “Comparative analysis of cytotoxic efect of aqueous cinnamon extract from Cinnamomum zeylanicum bark with commercial cinnamaldehyde on various cell lines,” Pharmaceutical Biology, vol. 47, no. 12, pp. 1174–1179, 2009.

[12] J. Lu, K. Zhang, S. Nam, R. A. Anderson, R. Jove, and W. Wen, “Novel angiogenesis inhibitory activity in cinnamon extract blocks VEGFR2 kinase and downstream signaling,” Carcinogenesis, vol. 31, no. 3, pp. 481–488, 20

[13] Abdeen and Samah, “Protective efect of cinnamon against acetaminophen- mediated cellular damage and apoptosis

in renal tissue," Environmental Science and Pollution Research, vol. 26, no. 1, pp. 240–249, 2017

[14] M. J. Ansari, D. Bokov, A. Markov et al., "Cancer combination therapies by angiogenesis inhibitors; a comprehensive review," Cell Communication and Signaling, vol. 20, no. 1, p. 49, 2022.

[15] S. S. Moselhy and H. K. Ali, "Hepatoprotective efect of cinnamon extracts against carbon tetrachloride induced oxidative stress and liver injury in rats," Biological Research, vol. 42, no. 1, pp. 93–98, 2009.

[16] C. M. Cabello, W. B. Bair, S. D. Lamore et al., "Te cinnamon-derived Michael acceptor cinnamic aldehyde impairs melanoma cell proliferation, invasiveness, and tumor growth," Free Radical Biology and Medicine, vol. 46, no. 2, pp. 220–231, 2009.

[17] A. Abdeen, A. Abdelkader, M. Abdo et al., "Protective efect of cinnamon against acetaminophen-mediated cellular damage and apoptosis in renal tissue," Environmental Science and Pollution Research, vol. 26, no. 1, pp. 240–249, 2019.

[18] Mosmann, Tim. "Rapid colorimetric assay for cellular growth and survival: application to proliferation and cytotoxicity assays" Journal of immunological methods 65, no. 1-2 (1983): 55-63.

[19] Marshall, N. J., C. J. Goodwin, and S. J. Holt. "A critical assessment of the use of microculture tetrazolium assays to measure cell growth and function." Growth regulation 5, no. 2 (1995): 69-84.

[20] 20) Kuan Liu, Peng-Cheng Liu, Run Liu, and Xing Wu. (2015). Dual AO/EB Staining to Detect Apoptosis in Osteosarcoma Cells Compared with Flow Cytometry. Med Sci Monit Basic Res :21: 15–20.

[21] Ramamoorthy Padmapriya, Loganathan Gayathri, Larance Ronsard, Mohammad. A Akbarsha, Ramasamy Raveendran (2017). In vitro anti-proliferative effect of Tephrosia purpurea on human hepatocellular carcinoma cells. Pharmacognosy magazine. 13: 49, 16-21.

[22] C. Ciniglia, G. Pinto, C. Sansone, A. Pollio (2010). Acridine orange/Ethidium bromide double staining test: A simple In-vitro assay to detect apoptosis induced by phenolic compounds in plant cells. Allelopathy Journal. 26 (2): 301-308.

[23] Maryam Mombeini, Ghasem Saki, Layasadat Khorsandi, ID and Neda Bavarsad (2018). Effects of Silymarin-Loaded Nanoparticles on HT-29 Human Colon Cancer Cells., medicina 1;1-9. doi:10.3390/medicina54010001.

[24] Krishnamoorthy Deepalakshmi, Sankaran Mirunalini. (2016). Antiproliferative and apoptotic effect of Pleurotus ostreatus on human mammary carcinoma cell line (michigan cancer foundation-7). 2: 4, 95-104.

[25] RK Rajeshkumar, R Vennila, S Karthikeyan, N Rajendra Prasad, M Arumugam, T Velpandian, T Balasubramaniam (2015). Antiproliferative activity of marine stingray Dasyatissephen venom on human cervical carcinoma cell line. Journal of Venomous Animals and Toxins including Tropical Diseases 21:41.